Low-Field Superconducting Phase of $(TMTSF)_2ClO_4$

F. L. Pratt,[1] T. Lancaster,[2] S. J. Blundell,[3] and C. Baines[4]

[1]*ISIS Facility, STFC Rutherford Appleton Laboratory, Chilton, Oxfordshire OX11 0QX, United Kingdom*
[2]*Centre for Materials Physics, Department of Physics, Durham University, South Road, Durham DH1 3LE, United Kingdom*
[3]*Department of Physics, Clarendon Laboratory, University of Oxford, Parks Road, Oxford OX1 3PU, United Kingdom*
[4]*Swiss Muon Source, Paul Scherrer Institut, Villigen CH-5232, Switzerland*

(Received 4 October 2012; revised manuscript received 4 January 2013; published 6 March 2013)

The low-field phase of the organic superconductor $(TMTSF)_2ClO_4$ is studied by muon-spin rotation. The zero temperature limit of the magnetic penetration depth within the TMTSF layers is obtained to be $\lambda_{ab}(0) = 0.86(2)$ μm. Temperature dependence of the muon-spin relaxation shows no indication of gap nodes on the Fermi surface nor of any spontaneous fields due to time-reversal-symmetry breaking. The weight of evidence suggests that the symmetry of this low-field phase is odd-frequency p-wave singlet, a novel example of odd-frequency pairing in a bulk superconductor.

DOI: 10.1103/PhysRevLett.110.107005 PACS numbers: 74.70.Kn, 74.20.Rp, 76.75.+i

The Bechgaard salts [1] $(TMTSF)_2X$ (anion X typically being PF_6 or ClO_4) attract continuing interest as a system whose rich physics is derived from a quasi-one-dimensional character and strong electron-electron interactions [2–4]. Although $(TMTSF)_2ClO_4$ (TMC) was the first ambient pressure organic superconductor (SC) to be discovered [5], the exact nature of its unconventional SC phases has yet to be resolved, with recent studies indicating that there is more than one distinct SC phase in this system. One phase is observed up to $\mu_0 H_{c2} = 0.16$ T for magnetic fields H oriented perpendicular to the TMTSF layers [2,6] [low-field superconductor (L-SC) phase], but aligning H within the TMTSF layers increases H_{c2} significantly above the Pauli limit [7] and allows a further high-field superconductor (H-SC) phase to be revealed. NMR finds clear evidence [8] for a field-induced transition between the L-SC phase and the second (H-SC) phase for fields above $\sim$1.5 T; the L-SC phase shows the Knight shift expected for a singlet state, whereas the H-SC does not, indicating a triplet state.

A fundamental parameter for a superconductor is the magnetic penetration depth λ, which determines the superfluid stiffness $\rho = c^2/\lambda^2$ characterizing the electromagnetic response to an applied magnetic field. The variation of $\rho(T)$ or $\lambda(T)$ with temperature T provides an important test of the gap symmetry. Previous estimates of $\lambda_{ab}(0)$ for TMC using muon-spin rotation (μSR) have either given a value around 1.2 μm [9–11] or a distinctly smaller value in the region of 0.5 μm [12]. None of these studies took into account the strong H variation of the linewidth due to the small value of H_{c2} when the supercurrents are in the ab plane. In order to resolve this $\lambda_{ab}(0)$ discrepancy and gain further information about the SC gap symmetry, we have made a detailed μSR study of this system, investigating the dependence of the SC properties over a full range of H and T.

From these results and other previously reported properties, we find strong evidence that the symmetry of the L-SC phase in TMC is an unusual odd-frequency pairing odd-parity singlet state. Odd-frequency pairing [13] was first proposed [14] for ^{3}He and subsequently for superconductors [15]. It is generally believed to be most relevant to symmetry-broken local environments, such as those near interfaces or in vortex cores [13], and has not previously been verified in a bulk superconductor.

Crystals of TMC form as needles aligned with the molecular stacking direction a. This is the most conducting direction of the material, which has a triclinic structure in which layers of TMTSF are arranged in the ab plane, separated along the c axis by layers of the ClO_4 anions. The c^* direction perpendicular to the molecular layers is the axis with the smallest conductivity. Our sample consisted of a mosaic of these crystals (total mass 124 mg) aligned with their a axes parallel. In the measurements, H is applied perpendicular to a, so we measure an axial average of the properties.

Transverse-field (TF) μSR provides a means of accurately measuring the internal magnetic-field distribution caused by the vortex lattice (VL) in a type-II SC [16] and has previously proven useful in establishing the vortex properties of molecular SCs [17,18]. Our field-cooled TF μSR measurements used two μ^+SR instruments. At the Swiss Muon Source within the Paul Scherrer Institute, we used the dilution refrigerator of the low temperature facility (LTF) instrument to measure down to 20 mK. At the ISIS Facility, STFC Rutherford Appleton Laboratory, UK, we used a ^{3}He sorption cryostat with the MuSR instrument to measure down to 300 mK. For the LTF measurements, the magnetic field $B_{\rm app} = \mu_0 H$ was applied perpendicular to both a and the plane of the sample mosaic. For the MuSR measurements, $B_{\rm app}$ was perpendicular to a and parallel to the plane of the sample mosaic. To ensure that the sample was in the nonmagnetic fully relaxed anion-ordered (AO) state, the cooling rate was maintained at 1 to 2 K h^{-1} between 35 and 15 K. All data analysis was carried out using the WIMDA program [19].

In TF μSR measurements performed above T_c, the distribution of field B at the muon $p(B)$ is broadened mainly by randomly oriented nuclear moments near the muon stopping sites, in this case dominated by the methyl groups at the ends of the TMTSF molecules. This leads to an essentially Gaussian relaxation of the muon polarization $P_x(t) \propto e^{-\sigma_n^2 t^2/2}\cos(\gamma_\mu\langle B\rangle t + \phi)$, where $\sigma_n^2 = \gamma_\mu^2\langle(B - \langle B\rangle)^2\rangle$. For $B_{\rm app} = 2.5$ mT, the TF broadening σ_n/γ_μ was monitored on cooling through the AO region and the width was found to reduce by about 10% on ordering. The AO doubles the b axis, leading to two inequivalent TMTSF stacks and significant distortion of the methyl groups on one of the stacks [20]. The observed change in σ_n is consistent with this distortion.

In the SC state, the VL gives a further broadening, i.e., $\sigma^2 = \sigma_n^2 + \sigma_{\rm VL}^2$, due to VL field width $B_{\rm rms} = \sigma_{\rm VL}/\gamma_\mu$. As the VL width here is very small, we did not attempt to spectrally resolve the asymmetric VL field profile as we did in previous studies of organic SC based on the BEDT-TTF (ET) molecule [2] such as κ-(ET)$_2$Cu(NCS)$_2$ [21,22] (κ-ET). The T dependence of $B_{\rm rms}$ and the shift of the average internal field $B_{\rm sh} = \langle B\rangle - B_{\rm app}$ at several values of $B_{\rm app}$ are shown in Fig. 1 (LTF data). Consistent results are obtained between runs on LTF and MuSR, despite the difference in orientation of $B_{\rm app}$, indicating a good axial average of the sample mosaic about the a axis. Both $B_{\rm rms}$ and $|B_{\rm sh}|$ fall continuously with increasing T, reaching zero above a characteristic temperature T'. The effect of increasing $B_{\rm app}$ is clearly seen as a depression of both T' and the size of the SC response measured by $B_{\rm rms}$ and $|B_{\rm sh}|$ at low T. In order to extract characteristic T' values, fits were made for $T < T'$ to a simple two-fluid T dependence, i.e., $1 - t^4$, where $t = T/T'$. The obtained values are shown in Fig. 1(c) for different values of H. There is an offset of around 0.2 K between values of T' obtained from $B_{\rm rms}$ and from $B_{\rm sh}$. Previous transport studies [6,23] suggested a vortex liquid phase just below T_c; we find that T' obtained from $B_{\rm rms}$ is well described by a 3D vortex melting curve and we assign this T' to the melting temperature T_m. The melting curve at low H takes the form [24] $T_m(H) = T_c(0)/[1 + (H/H_0)^{1/2}]$, where H_0 is a characteristic field. In highly 2D systems such as κ-ET, field-induced layer decoupling transitions dominate over 3D melting [18,22], but strong Josephson coupling for TMC stabilizes the layers against this decoupling.

Having established the stability of a VL phase over a range of T and $B_{\rm app}$, we focus on the accurate determination of λ. A reliable λ value can be obtained by measuring $B_{\rm rms}$ ($B_{\rm app}$) at low T and comparing with the prediction for an ideal vortex lattice calculated using the Ginzburg-Landau (GL) model [25]. The expected behavior is an increase of $B_{\rm rms}$ with increasing $B_{\rm app}$ in the region of B_{c1}, followed by a maximum and then a fall toward zero at B_{c2}. The measured $B_{\rm rms}$ ($B_{\rm app}$) at $T = 0.35$ K is shown in Fig. 2(a), along with the earlier reported results. For fitting the data, we assume an angular variation for ξ and λ of the form $(\cos^2\theta + \sin^2\theta/\gamma^2)^{-1/4}$, where θ is the angle to c^* and the anisotropy factor γ is obtained from the B_{c2} slope ratio [6] as $(2.3/0.11)^{1/2} = 4.5$. The overall behavior follows the GL form, consistent with a well-defined VL at low T. Data above 1 mT are fitted by the parameters $\lambda = 0.92(2)$ μm and $\kappa = 21(3)$. The corresponding B_{c2} value of 0.16(4) T is fully consistent with direct measurements [2,6]. The results of Refs. [10,11], which were made on aligned crystals with $B_{\rm app} \parallel c^*$, are also consistent with our fit, and our analysis includes these data. In contrast, the data points from Ref. [12] (deuterated sample) have an anomalously large $B_{\rm rms}$, suggesting incomplete

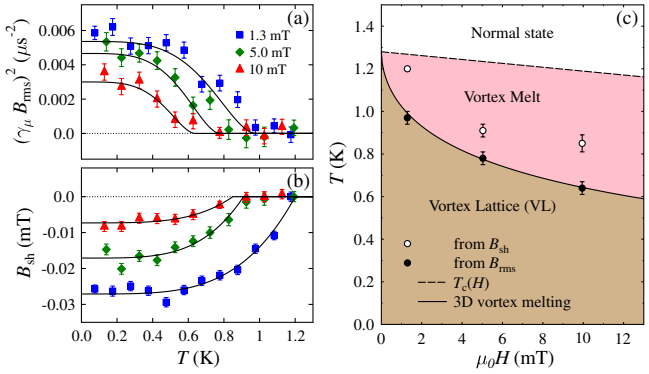

FIG. 1 (color online). (a) SC linewidth $B_{\rm rms}$ and (b) average field shift $B_{\rm sh}$ versus T for several different values of applied field measured using LTF. Characteristic transition temperatures T' are obtained from two-fluid model fits (lines). (c) The low-field phase diagram, comparing T' from μSR (points) with previously reported [6] $T_c(H)$ behavior for the $H \parallel c^*$ orientation that dominates here (dashed line). T' from $B_{\rm rms}$ is consistent with a 3D vortex melting curve (solid line) [24].

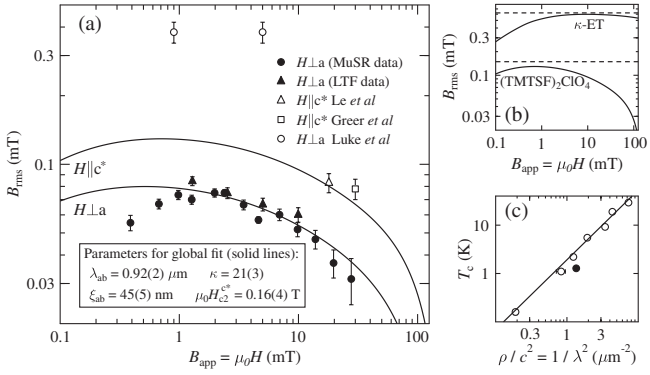

FIG. 2. (a) Field-dependent SC linewidth at 0.35 K (solid points). The open points are data taken from Refs. [10–12]. The global fit is described in the text (solid lines). (b) Comparison with $B_{\rm rms}(H)$ for the typical κ-ET organic superconductor. The dashed lines show the corresponding Barford-Gunn [49] field-independent values. (c) Scaling plot of T_c against $\rho(0)$ for molecular SCs. The filled point is the present result; open points are previous data for molecular SCs [35].

suppression of magnetism, and are excluded from the global fit. The small B_{c2} for $B_{\rm app} \parallel c^*$ leads to a remarkably strong field dependence of $B_{\rm rms}$ in our measurement range, and the extended plateau region typical of strong type-II (large κ) materials is not present here. In contrast, κ-ET [Fig. 2(b)] has a more well-developed plateau due to its larger values of κ and B_{c2}, along with an enhanced $B_{\rm rms}$ scale resulting from its smaller λ.

Breaking of time-reversal symmetry (TRS) in some types of unconventional SC can lead to spontaneous internal fields [26] in zero applied field (ZF). These weak fields have been observed by μSR in several examples, e.g., Sr_2RuO_4 [27] and more recently $LaNiC_2$ [28]. The spontaneous fields lead to an increase in the magnitude of the ZF depolarization rate of the muon polarization in the SC phase. To search for this effect, we took ZF μSR data as a function of T, scanning through T_c. Measured spectra were fitted to an exponential relaxation function $e^{-\lambda_{\rm ZF}t}$, and $\lambda_{\rm ZF}$ is shown in Fig. 3(a) (open circles). Within experimental error, we observe no evidence for a spontaneous local magnetic field, consistent with an earlier report on a deuterated sample [12].

In order to gain further information on the SC pairing symmetry present in TMC, we have examined the TF broadening down to 20 mK, taking relatively high statistics LTF data in a field of 1.9 mT. This field was chosen to be close to the maximum of $B_{\rm rms}$ and a field at which the VL is thermally stable over a wide range of T. The square of $\sigma_{\rm VL}(T)/\sigma_{\rm VL}(0)$ or equivalently $\rho(T)/\rho(0)$ is shown in Fig. 3(a) (solid points); each point corresponds to $\sim 10^7$ analyzed muon decay events. The observed reduction of

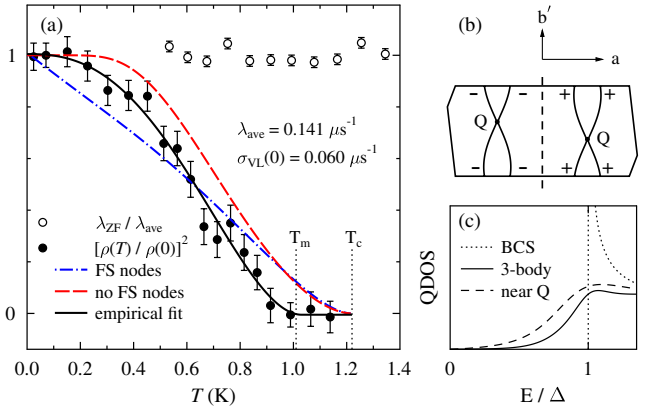

FIG. 3 (color online). (a) ZF relaxation rate (open circles). The solid points are TF data at 1.9 mT, plotted as $[\rho(T)/\rho(0)]^2 = [\sigma_{\rm VL}(T)/\sigma_{\rm VL}(0)]^2$ along with an empirical fit (solid line). The behavior expected for line nodes on the FS (dot-dashed line) is not seen, and the data are much closer to fully gapped BCS behavior (dashed line). (b) The AO state FS in the ab plane calculated by Nagai *et al.* [31] with subbands nearly degenerate at Q; our data are consistent with a gap function $\Delta(\mathbf{k})$ having a nodal plane parallel to the warped FS sheets (dashed line). (c) Illustration of the QDOS for different scenarios (see the text).

$\rho(T)$ with increasing T reflects the excitation of quasiparticles, which is highly sensitive to the quasiparticle density of states (QDOS) and thus the presence of any gap nodes on the Fermi surface (FS). A good description of the data is provided by the empirical power law $\rho(T)/\rho(0) = 1 - t^n (t = T/T_m)$. Our fitted value is $n = 2.5(3)$, which is not consistent with the $n = 1$ linear behavior predicted for models with FS line nodes and seen previously, for example, in μSR studies of κ-ET [17,29]. The clear saturation of $\rho(T)$ at low T is strongly indicative of a fully gapped SC without nodes on the FS. A nodal symmetry that would however be consistent with our data is a p_x state having a nodal plane running parallel to the FS [Fig. 3(b), dashed line]. This fully gapped state agrees with a previous thermal conductivity study [30] but differs from the conclusions of a recent ab plane angle-resolved heat capacity study [6], in which FS gap nodes were inferred [6,31] from the dip structure found in C/T data at 0.14 K and 0.3 T, when the field was oriented at $\pm 10°$ to a. These measurements may be reconciled with our result by noting that the anion subbands are nearly degenerate at Q [Fig. 3(b)], and thus the QDOS is expected to be strongly broadened by interband scattering at this point, reducing the effective gap [Fig. 3(c), dashed line]. This provides a mechanism for the quasiparticle "hot spot" that is needed to see angular structure in C/T, but the dominant point Q is actually a gap minimum here rather than a zero-crossing node.

From our $\rho(T)$ dependence, we can extrapolate to $T = 0$, giving $\lambda(0) = 0.86(2)$ μm. Scaling behavior $T_c \propto \rho^m$ has been explored for many classes of SC, including cuprates [32,33] and pnictides [34], where $m = 1$, and molecular systems [35], where $m = 3/2$. The new ρ value places TMC significantly below the molecular SC trend line [35] [Fig. 2(c)]. Introducing nonmagnetic impurities to TMC strongly suppresses T_c [36,37], but regular samples are extremely pure. The low T_c therefore suggests a different pairing mechanism from the other molecular SCs.

In order to systematically assign the SC phases, we summarize in Table I key experimental properties, both in the low-field L-SC state studied here and also in the high-field H-SC state established for in-plane fields above 1.5 T (Table I, upper two lines), along with the eight specific theoretical possibilities for a P-1 triclinic system with inversion symmetry, previously identified in the group theory analysis of Powell [38] (Table I, lower eight lines). For the L-SC phase, it can be seen that the only assignment consistent with the experiment is the OSO state (odd-frequency singlet with odd parity).

Although early theoretical studies suggested that such an odd-frequency SC would be intrinsically gapless [15], subsequent work has indicated that gapless behavior is not an essential feature. Models involving a condensate of composite bosons made up of a Cooper pair and a spin have been developed over many years [40,41]. The latest study coupled a Cooper pair and a magnon [41], and,

TABLE I. Properties of the superconducting states of TMC, experimental (top two lines) and theoretical (based on Powell [38]). Bold italic text marks our main conclusions and a unique assignment for L-SC. (E = even, O = odd, S = singlet, T = triplet, and HS = Hebel-Slichter.)

Symmetry (ω, S, k)	Type	Broken TRS	FS nodes[a]	Pauli limit	Knight shift	Disorder lowers T_c	HS peak	Label	Assignment
		No [12][b]	***No*** [30][b] Yes [6]	Untestable[c]	Yes [8]	Yes [36,37]	No [8,39]	L-SC	
		?	No [6]	No [7]	No [8]	?	No [8]	H-SC	
OSO	p singlet	No	No	Yes	Yes	Yes	No		***L-SC***
OTE	s polar	No	No	No	No	No	No		H-SC
OTE	s-β	Yes	No	No	No	No	No		
OTE	s-BW	No	No	No	Possible[d]	No	No		
ESE	s singlet	No	No	Yes	Yes	No	Yes		
ETO	p polar	No	No	No	No	Yes	No		H-SC
ETO	p-β	Yes	No	No	No	Yes	No		
ETO	p-BW	No	No	No	Possible[d]	Yes	No		

[a]Experimental result or symmetry requirement from theory.
[b]This study.
[c]L-SC to H-SC transition occurs first.
[d]Direction dependent.

depending on model parameters, the QDOS for this model could range from the standard sharply peaked form of the fully gapped Bardeen-Cooper-Schrieffer (BCS) model [Fig. 3(c), dotted line] through to a form with a completely closed gap. In an intermediate regime, the QDOS peak becomes broadened and weakened compared to BCS [Fig. 3(c), solid line]. As $\rho(T)$ falls faster than BCS in the region above 0.2 K (Fig. 3), this difference would be consistent with the broadening of the QDOS into the gap region expected for the intermediate regime in this type of model [41], although we note that thermal vortex motion could also lead to B_{rms} falling with T in a region just below T_m, giving an apparent extra fall in $\rho(T)$.

Turning to the H-SC phase, we see that there are two possibilities, either an *ETO* state of the polar form, as previously suggested by Powell [38], or alternatively an *OTE* state, also of polar form. *OTE* states have previously been discussed in the context of disordered 2D electron systems [42]. For a quasi-1D system such as we have here, a field-induced transition from *OSO* to *OTE* pairing is found in theoretical studies based on the extended Hubbard model, due to enhancement of charge fluctuations over spin fluctuations [43–45]. The two possible H-SC states could be distinguished by studying the effect of disorder on T_c within the H-SC phase, but such studies to date have only measured the L-SC phase [36,37].

Powell [38] has suggested a scenario in which the field-induced transition is due to spin-orbit coupling (SOC). In this picture, a strong SOC p-Balian-Werthamer (BW) state [38] for the L-SC phase crosses over to a weak SOC p-polar state [38] in the H-SC phase. For this to match the Knight shift data, the SOC must pin the **d** vector of the triplet state in a direction roughly midway between the a and b' axes, which does not correspond to any molecular axis. However, electron spin resonance studies of the TMTSF molecule in a range of environments [46] clearly show that the SOC always aligns with the molecular axes, which does not support this interpretation of the transition.

Finally, we note that the thermodynamic stability of odd-frequency bulk SCs was initially questioned, but recent theoretical work now concludes that these states should actually be stable [47,48]. The example identified here would suggest that such an odd-frequency state can indeed exist in a bulk material.

We thank N. Toyota for providing the sample, J. Quintanilla and M. Eschrig for discussions and comments, and EPSRC, UK, for financial support. We acknowledge the late E. H. Brandt for providing the numerical data to enable fitting to the GL model. Parts of this work were carried out at the STFC ISIS Facility, UK, and at the Swiss Muon Source, Paul Scherrer Institute, CH.

[1] D. Jérome, A. Mazaud, M. Ribault, and K. Bechgaard, J. Phys. (Paris), Lett. **41**, 95 (1980).
[2] T. Ishiguro, K. Yamaji, and G. Saito, *Organic Superconductors* (Springer, Berlin, 1998), 2nd ed.
[3] N. Toyota, M. Lang, and J. Müller, *Low-Dimensional Molecular Metals* (Springer, Berlin, 2007).
[4] *The Physics of Organic Superconductors and Conductors*, edited by A. G. Lebed (Springer, Berlin, 2008).
[5] K. Bechgaard, K. Carneiro, M. Olsen, F. B. Rasmussen, and C. S. Jacobsen, Phys. Rev. Lett. **46**, 852 (1981).
[6] S. Yonezawa, Y. Maeno, K. Bechgaard, and D. Jérome, Phys. Rev. B **85**, 140502(R) (2012).
[7] J. I. Oh and M. J. Naughton, Phys. Rev. Lett. **92**, 067001 (2004).
[8] J. Shinagawa, Y. Kurosaki, F. Zhang, C. Parker, S. E. Brown, D. Jérome, K. Bechgaard, and J. B. Christensen, Phys. Rev. Lett. **98**, 147002 (2007).

[9] D. R. Harshman and A. P. Mills, Jr., Phys. Rev. B **45**, 10 684 (1992).

[10] L. P. Le, A. Keren, G. M. Luke, B. J. Sternlieb, W. D. Wu, Y. J. Uemura, J. H. Brewer, T. M. Riseman, R. V. Upasani, L. Y. Chiang, W. Kang, P. M. Chaikin, T. Csiba, and G. Grüner, Phys. Rev. B **48**, 7284 (1993).

[11] A. J. Greer, D. R. Harshman, W. J. Kossler, A. Goonewardene, D. Ll. Williams, E. Koster, W. Kang, R. N. Kleiman, and R. C. Haddon, Physica (Amsterdam) **400**, 59 (2003).

[12] G. M. Luke, M. T. Rovers, A. Fukaya, I. M. Gat, M. I. Larkin, A. Savici, Y. J. Uemura, K. M. Kojima, P. M. Chaikin, I. J. Lee, and M. J. Naughton, Physica (Amsterdam) **326**, 378 (2003).

[13] Y. Tanaka, M. Sato, and N. Nagaosa, J. Phys. Soc. Jpn. **81**, 011013 (2012).

[14] V. L. Berezinskii, Pis'ma Zh. Eksp. Teor. Fiz. **20**, 628 (1974) [JETP Lett. **20**, 287 (1974)].

[15] A. Balatsky and E. Abrahams, Phys. Rev. B **45**, 13 125 (1992).

[16] J. E. Sonier, J. H. Brewer, and R. F. Kiefl, Rev. Mod. Phys. **72**, 769 (2000).

[17] F. L. Pratt, S. L. Lee, C. M. Aegerter, C. Ager, S. H. Lloyd, S. J. Blundell, F. Y. Ogrin, E. M. Forgan, H. Keller, W. Hayes, T. Sasaki, N. Toyota, and S. Endo, Synth. Met. **120**, 1015 (2001).

[18] T. Lancaster, S. J. Blundell, F. L. Pratt, and J. A. Schlueter, Phys. Rev. B **83**, 024504 (2011).

[19] F. L. Pratt, Physica (Amsterdam) **289–290**, 710 (2000).

[20] D. Le Pévelen, J. Gaultier, Y. Barrans, D. Chasseau, F. Castet, and L. Ducasse, Eur. Phys. J. B **19**, 363 (2001).

[21] S. L. Lee, F. L. Pratt, S. J. Blundell, C. M. Aegerter, P. A. Pattenden, K. H. Chow, E. M. Forgan, T. Sasaki, W. Hayes, and H. Keller, Phys. Rev. Lett. **79**, 1563 (1997).

[22] F. L. Pratt, S. J. Blundell, T. Lancaster, M. L. Brooks, S. L. Lee, N. Toyota, and T. Sasaki, Synth. Met. **152**, 417 (2005).

[23] S. Yonezawa, S. Kusaba, Y. Maeno, P. Auban-Senzier, C. Pasquier, and D. Jérome, J. Phys. Conf. Ser. **150**, 052289 (2009).

[24] E. H. Brandt, Rep. Prog. Phys. **58**, 1465 (1995).

[25] E. H. Brandt, Phys. Rev. B **68**, 054506 (2003).

[26] M. Sigrist and K. Ueda, Rev. Mod. Phys. **63**, 239 (1991).

[27] G. M. Luke, Y. Fudamoto, K. M. Kojima, M. I. Larkin, M. I. Larkin, J. Merrin, B. Nachumi, Y. J. Uemura, Y. Maeno, Z. Q. Mao, Y. Mori, H. Nakamura, and M. Sigrist, Nature (London) **394**, 558 (1998).

[28] A. D. Hillier, J. Quintanilla, and R. Cywinski, Phys. Rev. Lett. **102**, 117007 (2009).

[29] L. P. Le *et al.*, Phys. Rev. Lett. **68**, 1923 (1992).

[30] S. Belin and K. Behnia, Phys. Rev. Lett. **79**, 2125 (1997).

[31] Y. Nagai, H. Nakamura, and M. Machida, Phys. Rev. B **83**, 104523 (2011).

[32] Y. J. Uemura *et al.*, Phys. Rev. Lett. **62**, 2317 (1989).

[33] Y. J. Uemura, L. P. Le, G. M. Luke, B. J. Sternlieb, W. D. Wu, J. H. Brewer, T. M. Riseman, C. L. Seaman, M. B. Maple, M. Ishikawa, D. G. Hinks, J. D. Jorgensen, G. Saito, and H. Yamochi, Phys. Rev. Lett. **66**, 2665 (1991).

[34] M. J. Pitcher, T. Lancaster, J. D. Wright, I. Franke, A. J. Steele, P. J. Baker, F. L. Pratt, W. T. Thomas, D. R. Parker, S. J. Blundell, and S. J. Clarke, J. Am. Chem. Soc. **132**, 10 467 (2010).

[35] F. L. Pratt and S. J. Blundell, Phys. Rev. Lett. **94**, 097006 (2005).

[36] C. Coulon, P. Delhaes, J. Amiell, J. P. Manceau, J. M. Fabre, and L. Giral, J. Phys. (Paris) **43**, 1721 (1982).

[37] N. Joo, P. Auban-Senzier, C. R. Pasquier, P. Monod, D. Jérome, and K. Bechgaard, Eur. Phys. J. B **40**, 43 (2004).

[38] B. J. Powell, J. Phys. Condens. Matter **20**, 345234 (2008).

[39] M. Takigawa, H. Yasuoka, and G. Saito, J. Phys. Soc. Jpn. **56**, 873 (1987).

[40] P. Coleman, E. Miranda, and A. Tsvelik, Phys. Rev. Lett. **70**, 2960 (1993); Phys. Rev. B **49**, 8955 (1994); Phys. Rev. Lett. **74**, 1653 (1995).

[41] H. P. Dahal, E. Abrahams, D. Mozyrsky, Y. Tanaka, and A. V. Balatsky, New J. Phys. **11**, 065005 (2009).

[42] T. R. Kirkpatrick and D. Belitz, Phys. Rev. Lett. **66**, 1533 (1991); D. Belitz and T. R. Kirkpatrick, Phys. Rev. B **46**, 8393 (1992); **60**, 3485 (1999).

[43] H. Aizawa, K. Kuroki, and Y. Tanaka, Phys. Rev. B **77**, 144513 (2008).

[44] K. Shigeta, S. Onari, K. Yada, and Y. Tanaka, Phys. Rev. B **79**, 174507 (2009).

[45] K. Shigeta, Y. Tanaka, K. Kuroki, S. Onari, and H. Aizawa, Phys. Rev. B **83**, 140509(R) (2011).

[46] N. Kinoshita, M. Tokumoto, H. Anzai, T. Ishiguro, G. Saito, T. Yamabe, and H. Teramae, J. Phys. Soc. Jpn. **53**, 1504 (1984).

[47] D. Solenov, I. Martin, and D. Mozyrsky, Phys. Rev. B **79**, 132502 (2009).

[48] H. Kusunose, Y. Fuseya, and K. Miyake, J. Phys. Soc. Jpn. **80**, 054702 (2011).

[49] W. Barford and M. Gunn, Physica (Amsterdam) **156**, 515 (1988).